JPE 16-1-7

http://dx.doi.org/10.6113/JPE.2016.16.1.57
ISSN(Print): 1598-2092 / ISSN(Online): 2093-4718

Fault-Tolerant Strategy to Control a Reverse Matrix Converter for Open-Switch Faults in the Rectifier Stage

Eunsil Lee* and Kyo-Beum Lee†

*,†Department of Electrical and Computer Engineering, Ajou University, Suwon, Korea

Abstract

Reverse matrix converters, which can step up voltages, are suitable for applications with source voltages that are lower than load voltages, such as generator systems. Reverse matrix converter topologies are advantageous because they do not require additional components to conventional matrix converters. In this paper, a detection method and a post-fault modulation strategy to operate a converter as close as possible to its desired normal operation under the open-switch fault condition in the rectifier stage are proposed. An open-switch fault in the rectifier stage of a reverse matrix converter causes current distortions and voltage ripples in the system. Therefore, fault-tolerant control for open-switch faults is required to improve the reliability of a system. The proposed strategy determines the appropriate switching stages from among the remaining healthy switches of the converter. This is done based on reference currents or voltages. The performance of the proposed strategy is experimentally verified.

Key words: Carrier-Based Pulse Width Modulation (CB-PWM), Fault-detection, Fault-tolerant control, Open-switch fault, Reverse Matrix Converter (RMC)

I. INTRODUCTION

AC-AC conversion of electric power is widely employed in industrial applications, such as adjustable-speed drives (ASDs). Back-to-back converters (BBCs), which are the most common converters used in systems, have a DC link that includes energy storage components, such as a bulky capacitor for the voltage DC link or an inductor for the current DC link. However, matrix converters (MCs) do not utilize intermediate energy storage elements. MC topologies have many desirable features, such as a high power factor, a sinusoidal input current, a bi-directional power flow, and a compact design because of the lack of DC-link energy storage components [1], [2]. Conventional direct matrix converters (DMCs), which have an array of m × n bi-directional power switches to connect an m-phase source to an n-phase load, achieve voltage and current conversion in a single stage. Another type of MC investigated is the indirect matrix converter (IMC) or two-stage matrix converter [3]. The functions of IMCs are equivalent to those of DMCs. 3×3 IMCs are made up of a front-end three-phase to two-phase current source rectifier (CSR) and a rear-end voltage source inverter (VSI).

Despite these advantages, MCs have not yet gained much attention in industry because of several unsolved problems. The critical drawback of MCs is that the voltage transfer ratio between the input and the output has a maximum value of 86% in the linear modulation region. Several alternative topologies and modulation strategies have been designed to improve the voltage transfer ratio [4]-[6]. However, these methods require complex power circuits with complex control strategies. To boost the voltage without adding additional components, the reverse matrix converter (RMC) was presented in [7] and [8]. In these studies, it was determined that MCs can reverse the direction of power flow. In RMCs, the conventional voltage source stage is connected to a three-phase input source and the conventional current source stage is connected to a load.

Research to improve the reliability of systems using power converters has become increasingly important [9]-[12]. Systems that use switching devices must diagnose switching device faults and maintain their operation based on fault-tolerance controls. Methods for detecting open-switch

Manuscript received Apr. 25, 2015; accepted Jul. 22, 2015
Recommended for publication by Associate Editor Sangshin Kwak.
†Corresponding Author: kyl@ajou.ac.kr
Tel: +82-31-219-2376, Fax: +82-31-212-9531, Ajou University
*Dept. of Electrical and Computer Eng., Ajou University, Korea

faults in matrix converters are proposed in [13]-[15]. To detect and compensate for open-switch faults, additional components such as sensors and switches are used.

This paper proposes a detection and fault-tolerance control strategy based on a carrier-based PWM method for open-switch rectifier faults in an RMC. Open-switch faults are detected by using the current vector angle, and faulty switches can be identified by the phase angle. Then, the fault-tolerant control can be applied by simply revising the switching vector. The proposed tolerance control operates the RMC as close as possible to its desired normal operation. This method is easily implemented without adding any external components. Simulations and experiments are conducted to evaluate the performance and characteristics of the proposed fault detection and fault-tolerance control.

II. Reverse Matrix Converter

Generally, MCs are used in the buck mode operation. With this structure, the voltage transfer ratio cannot exceed 0.866 in the linear modulation region. RMCs can boost voltage without adding components to the conventional MC, and they allow inversion of the direction of power flow.

In an RMC, the traditional voltage source stage is connected to a three-phase input source and the traditional current source stage is connected to a load. Thus, the voltage source rectifier (VSR) acts as an active front-end rectifier. The zero voltage vector is applied to the VSR to boost the input voltage. The current source inverter (CSI) is modulated in the same way as the virtual DC-link voltage, which results in maximum output line-to-line voltages. This topology consists of a VSR and a CSI as shown in Fig. 1. The three phases of the source, designated as V_r, V_s and V_t, are connected to switches. The three load-side terminals are V_a, V_b and V_c. Filters are connected between the switches and the load. Like any other converter, matrix converters needs to be protected against the over-voltages and over-currents that might be destructive to their semiconductor devices. A protection circuit is made up of six diodes and a capacitor.

The boosting operation is explained as follows. The first state is called a "zero vector" and the control unit turns on or off all of the switches S_{rp}, S_{rp}, and S_{tp}. Accordingly, the *R*-phase, *S*-phase, and *T*-phase of the source are short-circuited via the inductors. As a result, the short-circuit current flows and the inductors store energy in the form of a magnetic field as shown in Fig. 2(a). Next, the other switching states are referred to as "active vectors." For example, the control unit turns off the switch S_{rp} and turns on the switch S_{rn}. Accordingly, the current is forced to flow through the ON switches and load as shown in Fig. 2(b). As a result, the total voltage available across the capacitor becomes larger than the source voltage by the EMF induced in the inductors. The capacitor voltage exceeds the source

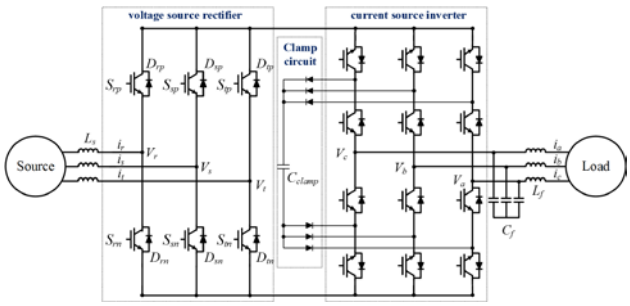

Fig. 1. Circuit of the reverse matrix converter system.

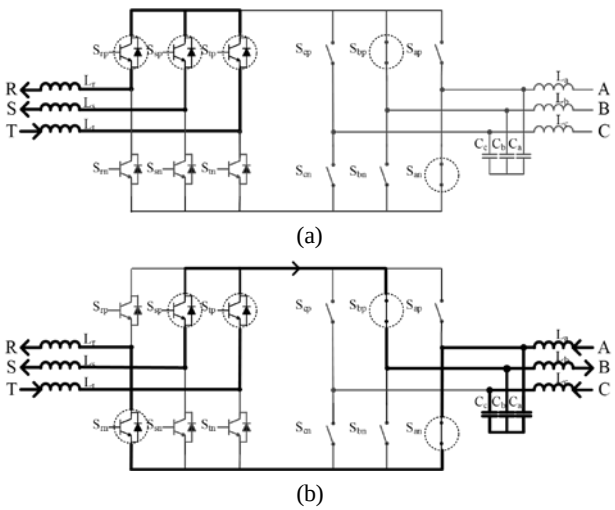

Fig. 2. Example of current paths of RMC for switching states (a) zero vector and (b) active vector.

voltage. As a result, the circuit acts as a boost chopper and the energy stored in the source inductors is released to the capacitors as electric energy. In this way, the control unit controls the switches to establish a current path from the source inductors to the filter capacitors. The commutation of the inverter stage can happen during the time when the zero vectors in the rectifier stage are applied to synthesize the reference input voltage vectors. Therefore, the rectifier stage can be switched to a free-wheeling state. Then the inverter stage can commutate with the zero dc link current. This has the added benefit of a reduction in the switching losses in the inverter stage by applying the zero dc link current commutation. Various modulation strategies can be applied to the RMC. However, a carrier-based PWM method is adopted in this paper [16].

III. Open-Switch Fault Analysis

The input and output of the MC are connected directly via semiconductor switches. Thus, distortions of the input are transmitted directly to the output waveforms. When an open-switch fault occurs in the rectifier stage, the input current, the DC-link voltage, and the output-side currents are distorted. An RL load composed of three resistors and three

inductors is used to demonstrate the proposed scheme. All open switch faults can distort the current in the rectifier and inverter stages of a reverse matrix converter. An open-switch fault in the *R*-phase leg is considered as an example in the following analysis.

Fig. 3 shows the waveforms when an open-switch fault occurs. S_{xp} in the upper switch fault prevents the partial zero vector state, where *x* (*r*, *s*, *t*). This means that the paths of the *x*-phase current are blocked, as indicated by the interval in Fig. 3. In such a case, the valid switching state "zero vector" is no longer possible, and the distorted *x*-phase current is in the interval of the blocked paths when the power factor of the rectifier is unity. The S_{xp} open-switch fault makes the inner circuit of the rectifier into an open circuit. In addition, the fault blocks the partial "active vector" switching state and affects the negative current, and the positive current remains nearly sinusoidal. Consequently, open-switch faults in the rectifier distort the current and voltage in the source and other sides.

The *R*-phase current is distorted in certain sections. Fig. 4 shows the voltage vector and its switching states in the *dq*-plane. The upper switch is on if it is a '1', and the lower switch is on if it is a '0'. The vectors are listed in the *R*, *S*, *T*-phase order. Thus, the vector $V_1(100)$ indicates that the switches S_{rp}, S_{sn}, and S_{tn} are in the on state at the same time.

If the switch S_{rp} is in the faulty state, the waveforms are distorted when S_{rp} is turned on and current flows in the negative direction. When the vector is on sectors 1 and 6, current flows through the diode D_{rp} or the switch S_{rn}, regardless of the switching state of switch S_{rp}. The fault type is classified into two groups: type 1, the zero vector region; and type 2, the zero and active vector region.

IV. Proposed Fault-Detection and Tolerant Control Method

There are six different current angle patterns cause by open-switch faults at different locations in a rectifier. The proposed detection method considers the current angle in the rectifier stage caused by an open-switch fault.

A. Fault Detection Method

The rectifier of an RMC is similar to the convectional PWM rectifier. Therefore, the conventional fault detection method for PWM rectifiers, presented in [9], can be employed. This method uses the derivative of the current vector angle to accurately determine the faulty switch.

In an examination of the fault detection method used by the rectifier of the RMC, it is assumed that an open-switch fault occurs in S_{rp} in an upper switch of the R-phase. Additionally, it is assumed that the input current provides a close-to-unity power factor and that power flows from the source to the load.

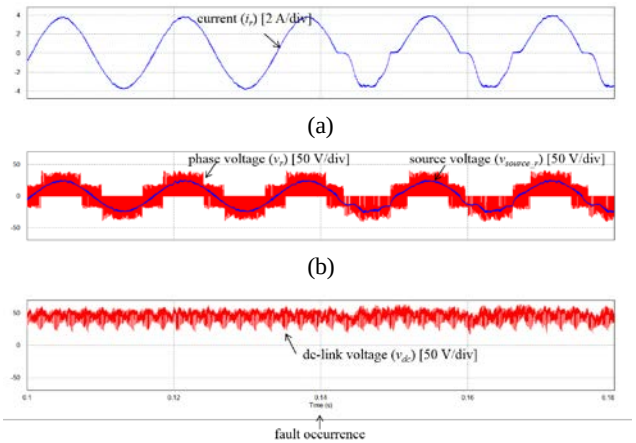

Fig. 3. (a) Input current, (b) voltage and (c) dc-link voltage under open-switch fault at S_{rp}.

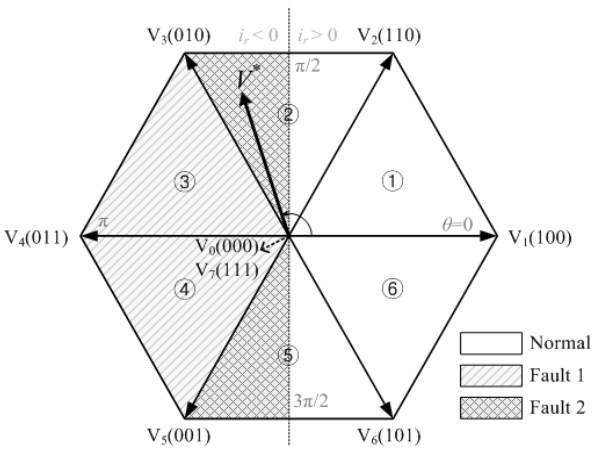

Fig. 4. Space voltage vector and switching states.

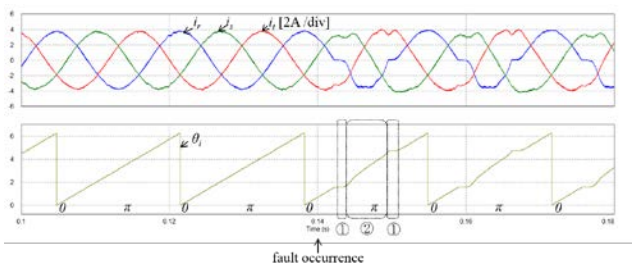

Fig. 5. Three-phase current and angle before and after the open-switch fault in S_{rp}.

The proposed fault detection method includes two steps. First, the input current vector angle is estimated. The current angle can be derived through the current of the stationary two-axis reference frame by following;

$$\theta_i = \begin{cases} tan^{-1}\left(i_{qs} / i_{ds}\right), & i_{ds} \geq 0, \\ tan^{-1}\left(i_{qs} / i_{ds}\right) + \pi, & i_{ds} < 0 \end{cases} \quad (1)$$

where:

$$i_{ds} = i_r,\ i_{qs} = \left(i_s - i_t\right) / \sqrt{3}\ .$$

Under normal conditions, the derivative of the input current vector angle is always constant and is equal to the source frequency times the sampling period. When a fault occurs in a switch, the derivative of the input current vector angle is distorted in certain sections. Thus, it is possible to detect whether an open switch fault occurs or not.

Second, the regions where the distorted angle occurs can identify the faulty switch. In the case of an open-switch fault in switch S_{rp}, the derivative of the input current vector angle is nearly zero at π/2 ~ 2π/3 and 4π/3 ~ 3π/2, as shown in Fig. 5. Table I shows the fault detection regions in which there was distortion. Thus, the fault can be identified as a switch S_{rp} open fault.

Utilizing a similar approach, it is possible to detect a faulty switch in the rectifier stage and to identify it as an open-switch fault. If multiple open-switch faults occur, it can be directly applied to the proposed diagnosis method. For example, it can be assumed that an open-switch fault occurs in S_{rp} and S_{rn} of the *R*-phase at the same time. In such a case, the distortion of the current angle is nearly zero at π/3~2π/3 and 4π/3~5π/3. This range shows an overlay in the range of the current distortion caused by the fault of the switches in Table I. Therefore, it is possible for the multiple open-switch faults to be diagnosed in the same way.

Fig. 6 shows a flowchart of the proposed open-fault detection method. The threshold values C_{th} and N_{th} have been chosen in accordance with the experience of the experimental work.

TABLE I
LOCATION OF OPEN-SWITCH FAULTS

Faulty switch	S_{rp}	S_{sp}	S_{tp}
Normal region	3π/2 ~ 2π 0 ~ π/2	π/6 ~ 7π/6	5π/6 ~ 11π/6
Type 1 region	2π/3 ~ 4π/3	4π/3 ~ 2π	0 ~ 2π/3
Type 2 region	π/2 ~ 2π/3 4π/3 ~ 3π/2	0 ~ π/6 7π6 ~ 4π/3	2π/3 ~ 5π/6 11π/6 ~ 2π
Current angle	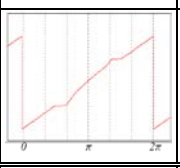	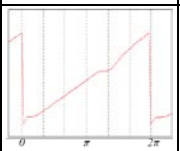	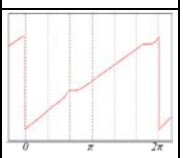
Faulty switch	S_{rn}	S_{sn}	S_{tn}
Normal region	π/2 ~ 3π/2	7π/6 ~ 2π 0 ~ π/6	11π/6 ~ 2π 0 ~ 5π/6
Type 1 region	5π/3 ~ 2π 0 ~ π/3	π/3 ~ π	π ~ 5π/3
Type 2 region	π/3 ~ π/2 3π/2 ~ 5π/3	π/6 ~ π/3 π ~ 7π/6	5π/6 ~π 5π/3 ~ 11π/6
Current angle	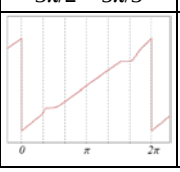	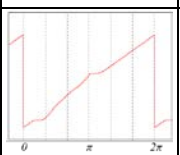	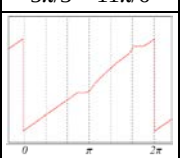

B. Fault-Tolerant Control Strategy

Implementation of the proposed fault-tolerant strategy involves replacement of the most appropriate switching states and calculation and their corresponding duty cycles.

Fig. 7 shows the sequence and the application time for all of the upper switches in the rectifier stage. To create the gate signal G_{xp} for the x-phase upper switch S_{xp}, two modulation signals $M_{x(y)}$ and a carrier signal are needed where $x \in (r, s, t)$ and $y \in (1, 2)$. The *x*-phase lower switch state is complementary to that of the upper switch.

$$M_{x(1)} = \frac{\left(-2(1-d_\alpha)\frac{v_x^* + v_{sn}^*}{v_{dc}} + d_\alpha + 1\right)}{2},$$
$$M_{x(2)} = \frac{\left(-2d_\alpha\frac{v_x^* + v_{sn}^*}{v_{dc}} - (1-d_\alpha) + 1\right)}{2} \quad (2)$$

where, v_{dc} is the average value of the DC-link voltage in one sampling period, the v_x^* values are the reference input phase voltages of the source, and v_{sn}^* is the offset voltage. d_α is the duty cycle of the inverter stage in the RMC. It is used to synchronize the switching of the rectifier stage and the inverter stage.

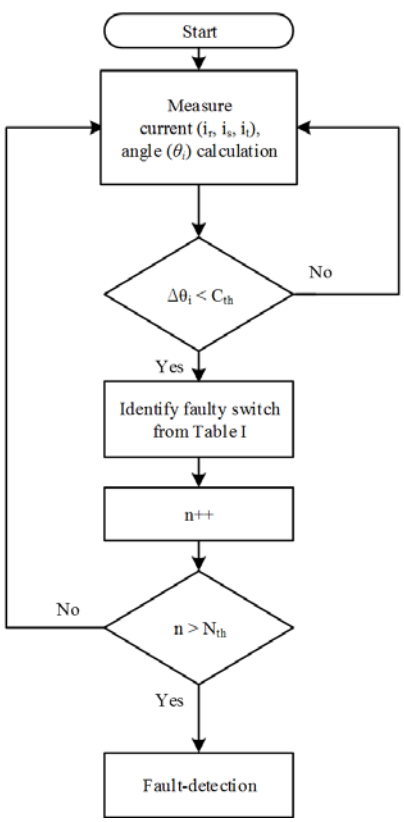

Fig. 6. Flowchart of the proposed open-fault detection.

From eq. (2), the gate signal G_{xp} can be obtained by:

$$G_{x(y)} = \begin{cases} 1, & M_{x(y)} \geq M_{tri}, \\ 0, & M_{x(y)} < M_{tri}, \end{cases} \qquad G_{xp} = G_{x(1)} \overline{XOR}\ G_{x(2)}. \tag{3}$$

Type 1: When an open-switch S_{rp} fault occurs in the rectifier stage, in the region of $2\pi/3 \sim 4\pi/3$, the errors between the desired voltages and the actual voltages increase because the zero vector $V_7(111)$ is converted into an active vector $V_4(011)$. Thus, this situation can be resolved by replacing the zero vector $V_7(111)$ with another zero vector $V_0(000)$. The fault can be perfectly compensated with a duty cycle of the active vector that is the same as the conventional one.

After the detection of a fault, the modulation signals are revised to:

$$M_{x(1)}' = M_{x(1)} + \alpha_1, \qquad M_{x(2)}' = M_{x(2)} - \alpha_2 \tag{4}$$

where:

$$\alpha_1 = 1 - M_{r(1)}, \alpha_2 = M_{r(2)}.$$

Fig. 7 shows the revised switching states for the proposed fault-tolerant method. In this case, the sequence of switching is changed from $V_7(111)$-$V_4(011)$-$V_5(001)$-$V_0(000)$ to $V_4(011)$- $V_5(001)$-$V_0(000)$.

Type 2: When an open-switch S_{rp} fault occurs in the rectifier stage, in the region of $\pi/2 \sim 2\pi/3$ or $4\pi/3 \sim 3\pi/2$, the waveforms of the current are significantly distorted. In this case, the vectors $V_6(101)$ and $V_7(111)$ are converted into $V_5(001)$ and $V_4(011)$, respectively. In the first step, $V_7(111)$ can be replaced by $V_0(000)$ in a similar way to that used for type 1 faults. Next, the $V_6(101)$ vector can be replaced by the nearest available vector based on the reference voltage vector by projecting it orthogonally onto vector $V_5(001)$, as shown in Fig. 8. Thus, the application time for the vector $V_5(001)$ is added to half of the application time of $V_6(101)$. Finally, the modulation signals are revised as follows;

$$\begin{aligned} M_{r(1)}' &= M_{r(1)} + \alpha_1 + \beta_1, & M_{r(2)}' &= M_{r(2)} - \alpha_2 - \beta_2, \\ M_{s(1)}' &= M_{s(1)} + \alpha_1, & M_{s(2)}' &= M_{s(2)} - \alpha_2, \\ M_{t(1)}' &= M_{t(1)} + \alpha_1 + \beta_1 / 2, & M_{t(2)}' &= M_{t(2)} - \alpha_2 - \beta_2 / 2 \end{aligned} \tag{5}$$

where:

$$\alpha_1 = 1 - M_{s(1)}, \beta_1 = M_{s(1)} - M_{r(1)},$$
$$\alpha_2 = M_{s(2)}, \beta_2 = M_{r(2)} - M_{s(2)}.$$

Fig. 9 shows the revised switching states for the proposed fault-tolerant method. In this case, the sequence of switching is changed from $V_7(111)$-$V_6(101)$-$V_5(001)$-$V_0(000)$ to $V_5(001)$- $V_0(000)$.

V. Simulation and Experimental Results

To verify the efficiency of the proposed method, a simulation and experimental test bed has been developed. The simulation studies are conducted in the PSIM software environment. The system introduced in Section II was built, and Fig. 10 shows actual pictures of the power converter and control unit. The two-pack IGBT module (Hivron, X2G50SD12P1), which consists of two IGBTs and two antiparallel diodes, is used to configure the rectifier stage. The system is controlled by a control unit, which is implemented with a DSP (TI, TMS320C28346), an FPGA (Xilinx, XC6SLX45CSG324), and other peripheral circuits. The input of the converter is connected to the grid through a three-phase variac. An LC filter is connected at the output side of the converter to attenuate the harmonics, and a clamp circuit is used to protect the switch devices. Details of the system parameters are shown in Table II. Referring to the vector control block diagram in Fig. 11, two PI controllers are used

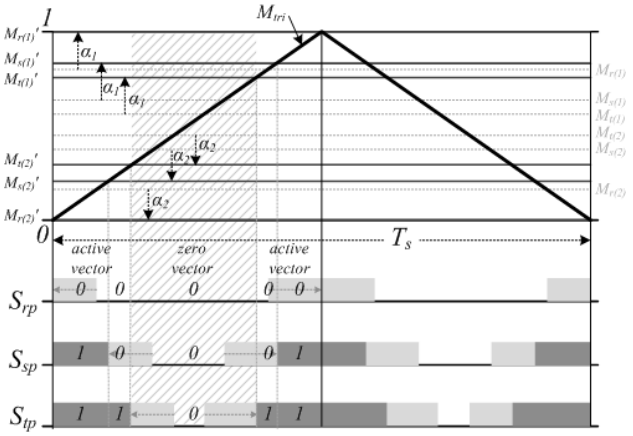

Fig. 7. Revised switching states for type 1 fault.

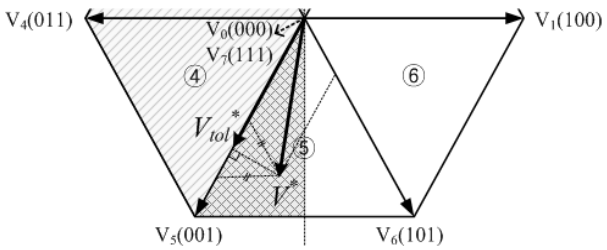

Fig. 8. Reference and compensated voltage vector.

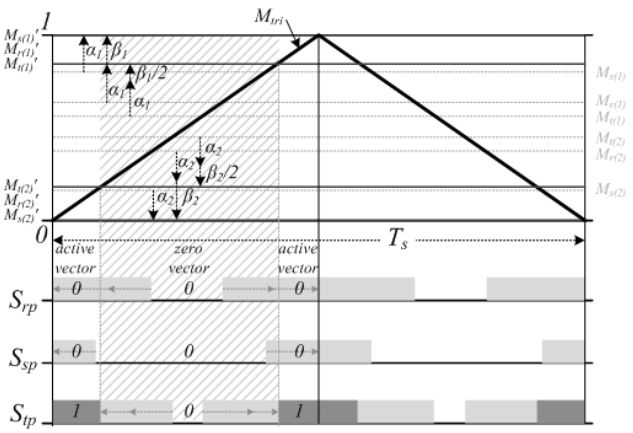

Fig. 9. Revised switching states for type 2 fault.

TABLE II
SYSTEM PARAMETERS

Filter capacitors speed	7 μF
Filter inductors	1.3 mH
R-L load	10 Ω/1 mH
Sampling period	100 μs
Switching frequency	20 kHz

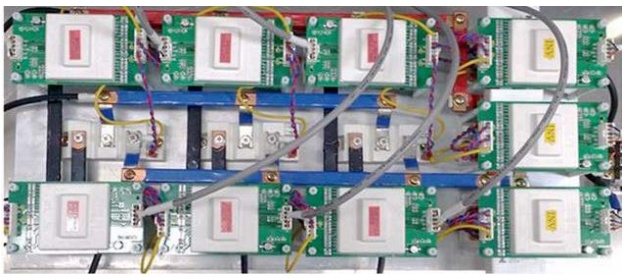

(a)

(b) (c)

Fig. 10. Experimental set of RMC (a) power board, (b) control board and (c) sensors, etc.

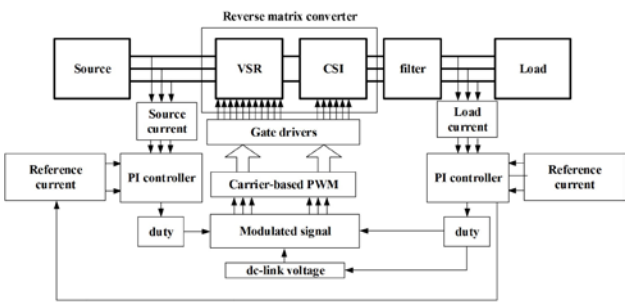

Fig. 11. Block diagram of the control scheme for the RMC system.

for controlling the current of the source and the load.

Fig. 12 and Fig. 13 show the simulation and experimental steady-state waveforms with the carrier-based PWM strategy. The reference current at the output is constant. The voltage at the load side is larger than the voltage at the source side. The phase currents and voltages are roughly sinusoidal.

Fig. 14 and Fig. 15 show the simulation and experimental results of an RMC operating with the proposed fault detection method when the switch S_{rp} in the rectifier stage is subjected to an open-circuit failure. If the current is large, the distortion of the current is remarkable. In this case the fault diagnosis is easy. In this paper, experiments were performed by selecting the magnitude of an appropriate current, and the performance

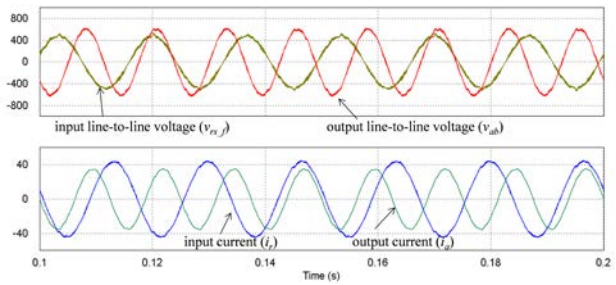

Fig. 12. Simulated waveforms of RMC with boosting operation.

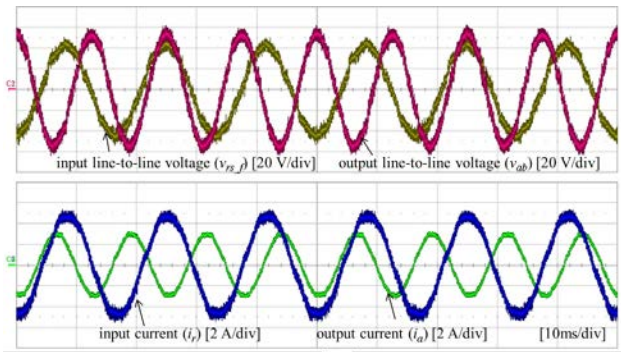

Fig. 13. Experimental waveforms of RMC with boosting operation.

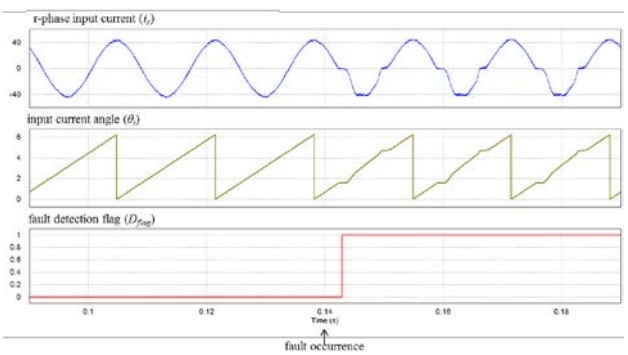

Fig. 14. Simulated waveforms with the proposed fault detection method.

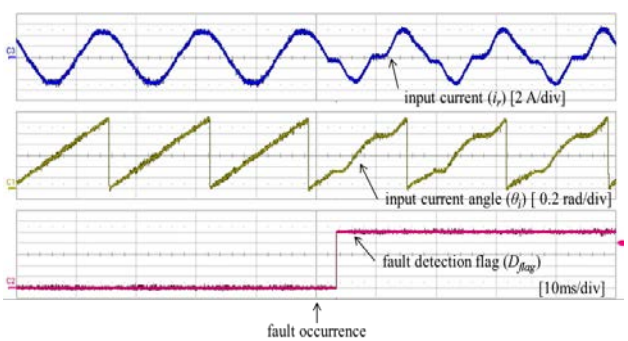

Fig. 15. Experimental waveforms with the proposed fault detection method.

of the proposed method under a large current was verified using simulation results. An open-switch fault is detected based on the monitoring of the input currents. The two-step algorithm is developed to identify faulty switches. If the

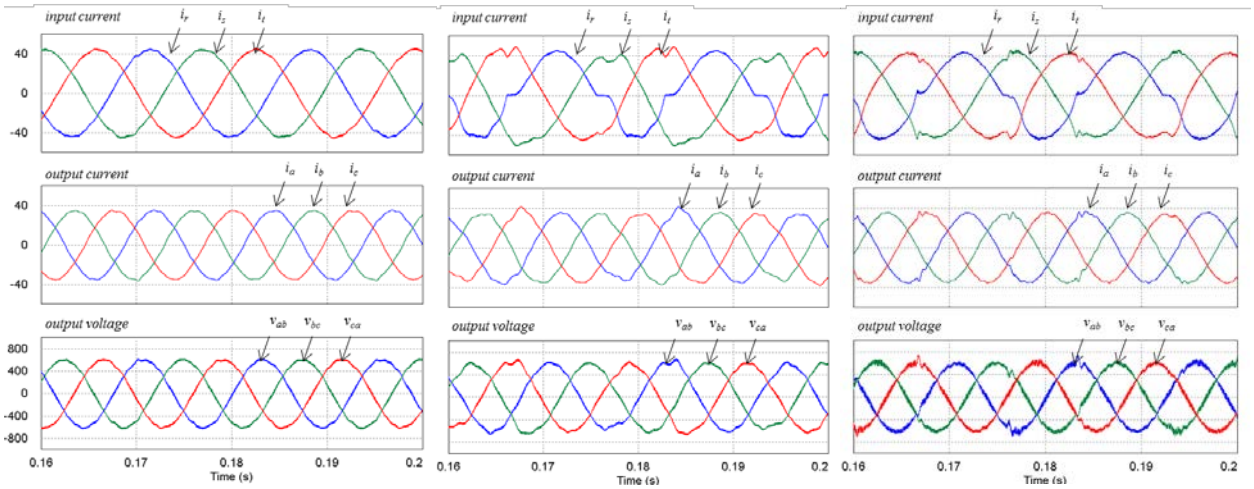

(a) (b) (c)

Fig. 16. Simulated waveforms with (a) normal condition, (b) switch S_{rp} open-fault condition and (c) fault-tolerant control.

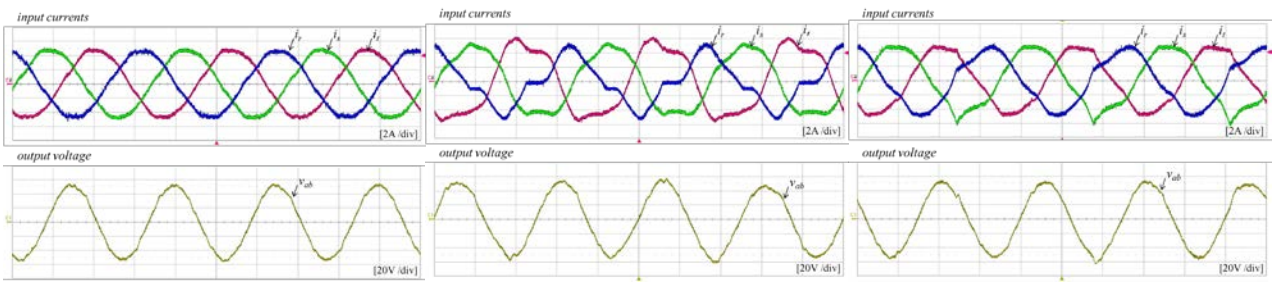

(a) (b) (c)

Fig. 17. Experimental waveforms with (a) normal condition, (b) switch S_{rp} open-fault condition and (c) fault-tolerant control.

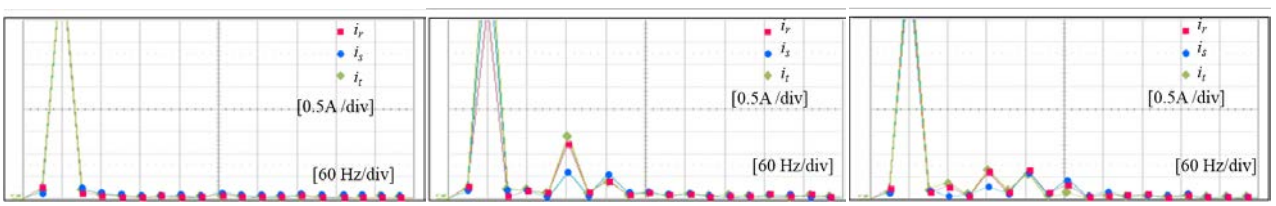

(a) (b) (c)

Fig. 18 Experimental harmonic spectrum of the three-phase input currents (a) normal condition, (b) switch S_{rp} open-fault condition and (c) fault-tolerant control.

switch S_{rp} is faulty, then the *R*-phase current will become distorted, which causes distortions in the output voltage and current. The variation in the current angle is not kept constant in the distorted regions. In this case, the current angle is nearly zero in the $\pi/2 \sim 2\pi/3$ and $4\pi/3 \sim 3\pi/2$ regions. Thus, the faulty switch can be identified as the switch S_{rp} using the flowchart in Fig. 6.

The effectiveness of the proposed strategy can be verified by Fig. 16. It shows the three-phase input currents, output currents and output voltages both before and after applying the fault tolerant control when the switch S_{rp} open-fault occurs in the rectifier stage.

When the proposed fault-tolerant strategy is activated, the distortion in the three-phase input currents is reduced. During the fault-tolerant operation, a revised switching state is

TABLE III
EXPERIMENTAL RESULT

Condition		Normal	Open-switch fault	Fault-tolerant method
current THD [%]	i_r	2.7	36.4	19.5
	i_s	3.1	25.9	17.8
	i_t	3.3	16.3	17.3
power factor		0.99	0.92	0.97

applied such that the error in the input current is minimized. The corresponding experimental results are presented in Fig. 17. It can be seen that they closely match the simulation results.

To investigate the performance of the proposed strategy in terms of power quality, the harmonic spectrum (FFT: Fast Fourier Transform), the total harmonic distortion (THD) content of the input currents, and the power factor when the converter operates under normal and faulty conditions both with and without the proposed tolerant control are presented in Fig. 18 and Table III. It can be seen that the third harmonic is present for the open-switch faults. This third harmonic results from the interaction of the fundamental frequency current in the source and the negative sequence current in the input phases. Therefore, the location of the open circuit fault is based on detecting the input current. As shown in the Fig. 18 and Table III, by employing the proposed fault-tolerant strategy, the harmonic spectra, the THD content of the input current, and power factor under an open-switch fault are significantly improved.

VI. CONCLUSION

This paper proposed an open-switch fault-detection method and a fault-tolerant control strategy for the rectifier in a reverse matrix converter. The proposed detection method can identify which switch is in the open-switch fault state in the converter. Based on the replacement of the switching vector, the reverse matrix converter can compensate for the open-switch fault. The proposed method does not need additional components. Therefore, it is suitable for implementation in simple systems. Moreover, the proposed method improves the current THD and power factor at the input-side.

ACKNOWLEDGMENT

This work was supported by the Basic Science Research Program through the National Research Foundation of Korea (NRF) funded by the Ministry of Education (No. 2013R1A1A2A10006090).

REFERENCES

[1] T. Friedli, J. W. Kolar, J. Rodriguez, and P. W. Wheeler, "Comparative evaluation of three-phase ac–ac matrix converter and voltage dc-link back to-back converter systems," *IEEE Trans. Ind. Electron*., Vol. 59, No. 12, pp. 4487-4510, Dec. 2012.

[2] J. W. Kolar, T. Friedli, J. Rodriguez, and P. W. Wheeler, "Review of three-phase PWM ac-ac converter topologies," *IEEE Trans. Ind. Electron.—Special Section Matrix Converters*, Vol. 58, No. 11, pp. 4988-5006, Nov. 2011.

[3] K. Iimori, K. Shinohara, O. Tarumi, Z. Fu, and M. Muroya, "New current-controlled PWM rectifier-voltage source inverter without DC link components," *in Proc. Power Conversion Conf*., pp. 783-786, 1997.

[4] K. Park, K. B. Lee, and F. Blaabjerg, "Improving output performance of a Z-source sparse matrix converter under unbalanced input-voltage conditions," *IEEE Trans. Power Electron*., Vol. 27, No. 4, pp. 2043-2054, Apr. 2012.

[5] B. Ge, Q. Lei, W. Qian, and F. Z. Peng, "A family of Z-source matrix converters," *IEEE Trans. Ind. Electron*., Vol. 59, No. 1, pp. 35-46, Jan. 2012.

[6] T. Wijekoon, C. Klumpner, P. Zanchetta, and P. W. Wheeler, "Implementation of a hybrid AC–AC direct power converter with unity voltage transfer," *IEEE Trans. Power Electron*., Vol. 23, No. 4, pp. 1918-1926, Jul. 2008.

[7] X. Liu, P. C. Loh, P. Wang, F. Blaabjerg, Y. Tang, and E. A. Al-Ammar, "Distributed generation using indirect matrix converter in reverse power mode," *IEEE Trans. Power Electron*., Vol. 28, No. 3, pp. 1072-1082, Mar. 2013.

[8] X. Liu, P. Wang, P. C. Loh, and F. Blaabjerg, "Distributed generation interface using indirect matrix converter in boost mode with controllable grid side reactive power," in *Proc. IPEC*, pp. 59-64, 2012.

[9] W. S. Im, J. M Kim, D. C. Lee and K. B. Lee, "Diagnosis and Fault Tolerant Control of 3-phase AC-DC PWM Converter Systems," *IEEE Trans. Ind. Appl*., Vol. 49, No. 4, pp. 1539-1547, Jul./Aug. 2013.

[10] W. S. Im, J. S. Kim, J. M. Kim, D. C. Lee and K. B. Lee, "Diagnosis Methods for IGBT Open Switch Fault Applied to 3-Phase AC/DC PWM Converter," *Journal of Power Electronics*, Vol. 12, No. 1, pp. 120-127, Jan. 2012.

[11] J. S. Lee and K. B. Lee, "Tolerance Control for Inner Open-Switch Faults of a T-type Three-Level Rectifier," *Journal of Power Electronics*, Vol. 14, No. 6, pp. 1157-1165, Nov. 2014.

[12] Y. Ko, K. B. Lee, D. C. Lee, and J. M. Kim, "Fault Diagnosis of Three-Parallel Voltage-Source Converter for a High-Power Wind Turbine," *IET Power Electron*., Vol. 5, No. 7, pp. 1058-1067, Aug. 2012.

[13] S. Khwan-on, L. Lillo, L. Empringham, and P. Wheeler, "Fault-tolerant matrix converter motor drives with fault detection of open switch faults," *IEEE Trans. Ind. Electron*., Vol. 59, No. 1, pp. 257-268, Jan. 2012.

[14] S. Kwak, "Four-leg-based fault-tolerant matrix converter schemes based on switching function and space vector methods," *IEEE Trans. Ind. Electron*., Vol. 59, No. 1, pp. 235-243, Jan. 2012.

[15] E. Lee and K. B. Lee, "Fault diagnosis for a sparse matrix converter using current patterns," in *Proc. APEC*, pp. 1549-1554, 2012.

[16] T. D. Nguyen and H.-H. Lee, "Dual three-phase indirect matrix converter with carrier-based PWM method," *IEEE Trans. Power Electron*., Vol. 29, No. 2, pp. 569-581, Feb. 2014.

Eunsil Lee received her B.S. and M.S. degrees in Electrical and Computer Engineering from Ajou University, Suwon, Korea, in 2010 and 2012, respectively, and the Ph.D. degree in Electrical and Computer Engineering from Ajou University, Suwon, Korea, in 2015. Her current research interests include ac-ac power converter systems, multilevel inverters, and the operation of motor drives.

Kyo-Beum Lee received his B.S. and M.S. degrees in Electrical and Electronics Engineering from Ajou University, Suwon, Korea, in 1997 and 1999, respectively; and his Ph.D. degree in Electrical Engineering from Korea University, Seoul, Korea, in 2003. From 2003 to 2006, he was with the Institute of Energy Technology, Aalborg University, Aalborg, Denmark. From 2006 to 2007, he was with the Division of Electronics and Information Engineering, Chonbuk National University, Jeonju, Korea. In 2007, he joined the School of Electrical and Computer Engineering, Ajou University. His current research interests include electric machine drives, renewable power generation, and electric vehicle applications.